Location of Mesoporphyrin in Liposomes Determined by Site-Selective Fluorescence Spectroscopy

ARTICLE *in* THE JOURNAL OF PHYSICAL CHEMISTRY B · JUNE 2009

Impact Factor: 3.3 · DOI: 10.1021/jp9022184 · Source: PubMed

Location of Mesoporphyrin in Liposomes Determined by Site-Selective Fluorescence Spectroscopy

Levente Herenyi,* Dániel Veres, Sándor Békási, István Voszka, Károly Módos, Gabriella Csík, András D. Kaposi, and Judit Fidy

Department of Biophysics and Radiation Biology, Semmelweis University, P. O. Box 263, H-1444 Budapest, Hungary

Received: March 12, 2009; Revised Manuscript Received: April 8, 2009

Binding of photosensitizers to target cells is a crucial step during the photodynamic effect. Sensitizer distribution is a good indication of whether the chemical is a good candidate for perturbing cell membrane integrity. Hence, the photophysical properties of porphyrinoid sensitizers in microheterogeneous systems such as liposomes are of outstanding interest. Here we present a site-selective fluorescence study of liposome systems. Monocomponent, small unilamellar vesicles formed of different phosphatidylcholines with incorporated mesoporphyrin were investigated. The size distribution of liposomes was measured by dynamic light scattering after each step of the experiment. On the basis of fluorescence line narrowing spectra of mesoporphyrin, the inhomogeneous distribution function was determined in order to characterize the photosensitizer location. The dual character of the functions revealed two different locations. Decomposition of the inhomogeneous distribution functions into Gaussians and the analysis of the fit results suggest that one of the locations for mesoporphyrin is between the two lipid layers, and the other one is between the hydrocarbon chains of the lipid molecules.

Introduction

The ability of photosensitizers to generate reactive oxygenated products is considered to be fundamental for photodynamic applications. Almost all sensitizers studied in this context belong to the group of porphyrin derivatives. This class of substances is efficient in the formation of very toxic short-lived species following irradiation with light in the presence of oxygen. The presence of these highly reactive species in a cellular environment may lead to the degeneration or disintegration of biological structures such as cellular membranes. The most important application of photosensitizers is the destruction of malignant tumors by photodynamic therapy (PDT). They are used in tumor diagnostics as well. Photodynamic methods have also been considered for the inactivation of viruses.[1−6]

The observed ambiguous connection between the intrinsic properties of a sensitizer and its photodynamic effectiveness turned attention to the influence of the biological environment.[7] To become photodynamically active, the sensitizer needs to be closely associated with the target. Usually, molecular association is made possible through the simultaneous cooperation of several weak interactions. Consequently, the favorable pattern of location depends on the nature of the sensitizer and on the complex environmental conditions as well. Knowing the distribution of the sensitizer associated with the target cells can help to predict the outcome of a photodynamic reaction. On the basis of this information one can decide whether a sensitizer may be considered as a good candidate for affecting the integrity of the cell membrane by a photodynamic effect.

Liposomes are often used as simple models for mimicking cellular membranes. Noncovalent interactions of the sensitizer with surrounding molecules in such systems have been explored in several papers.[8,9] Porphyrins in the presence of liposomes, and the changes of their photophysical parameters, have also been studied.[10−13] The change of photophysical properties proved to be a useful tool for getting information on the location of porphyrin molecules and on the nature of interactions. Several publications report on the distribution of porphyrins in the various compartments of liposomes based on different fluorescence experimental techniques.[14−16] In numerous articles the vertical location of the photosensitizers in the bilayer has been studied, and some papers demonstrated a direct correlation between the location depth and photosensitizing activity.[17−19]

Generally, the properties relevant to the interactions may be revealed from the optical spectra of dye molecules, just as in the case of porphyrins. In conventional spectra, besides temperature-induced homogeneous broadening, slight fluctuations of the surrounding matrix lead to inhomogeneity in the chromophore environment and cause broadening of the spectral bands. This large inhomogeneous broadening makes it impossible to use the results of regular spectroscopic measurements for the interpretation of finer effects. Energy-selected or site-selective fluorescence spectroscopy is a high-resolution method capable of monitoring the environmental effects free of inhomogeneous broadening. General discussion of this technique has appeared in numerous papers and reviews.[20−22] It has been shown that the method may also be successfully used to study the effect of the surrounding matrix on biomolecules such as proteins.[23,24]

The basic principles of this technique are the following. Fluorescence emission spectra are measured on samples which are cooled from room temperature to cryogenic temperatures. As a consequence of the cooling, the sites populated at room temperature freeze in the sample. This information, as a snapshot, is conserved and can be studied by spectroscopy.[22] The meaning of the term "site" in this context is a molecular environment (almost without fluctuations) of the dye molecule as well as a detuned electronic transition energy (characterized

* To whom correspondence should be addressed. Phone/Fax: 36-1-266-6656. E-mail: levente.herenyi@eok.sote.hu.

10.1021/jp9022184 CCC: $40.75
Published on Web 05/01/2009

by a certain wavenumber or wavelength) of the dye molecule in this environment. With the use of narrow bandwidth on the excitation side (laser or a sufficiently good monochromator), part of the molecules will be simultaneously but selectively excited. This subpopulation (in electronic transition energy) of the chromophores corresponds to such a specific frozen environment. Thus the sites are defined in this sense. Because of the selective excitation, the emission spectra consist of sharp emission lines (line narrowing) resulting from resonant excitations, superimposed on the background of broad bands which are also present, due to the emissions from nonresonant (phonon-coupled) excitations.[22] The mth line originates from the transition between the lowest vibrational level of the first electronic excited state (1,0) and the ground state (0,0) after an excitation of (1,m) $\rightarrow$ (0,0) and a vibrational relaxation (1,m) $\rightarrow$ (1,0). If the background has been subtracted from the spectra, the line intensity, I_m, is given by the formula

$$I_m = KI_{\mathrm{exc}}AB_mN_m(\nu,\Delta\nu) \quad (1)$$

where K is a constant, I_{exc} is the excitation intensity, A is the fluorescence emission probability, B_m is the absorption transition probability, and $N_m(\nu,\Delta\nu)$ denotes the number of selectively excited molecules at a given excitation frequency (ν) that naturally depends on the excitation bandwidth ($\Delta\nu$) as well.[25] We may adopt the simplest phenomenological model of inhomogeneous broadening, assuming that the inhomogeneity does not influence the vibrational levels of a given electronic state (one-dimensional inhomogeneity).[26] In this case, all the $N_m(\nu)$ functions, as cumulative distribution functions, have the same common form, shifted along the frequency scale. Thus, any one of them can characterize the inhomogeneous broadening. Let us choose the $N_0(\nu)$ function which is a possible representation of the so-called inhomogeneous distribution function (IDF). Since the origin of the inhomogeneous broadening is the various chromophore environments, this function is characteristic for the site distribution of chromophore molecules in their environments. (The IDF in density function representation [$N^*(\nu) = \mathrm{d}N_0(\nu)/\mathrm{d}\nu$] can be regarded also as the true (1,0)$-$(0,0) band shape characterizing both the absorption and the fluorescence emission broadened only by inhomogeneities.)

In the present work we investigated monocomponent, small, unilamellar vesicles (SUVs) formed by three kinds of phospholipids, namely dimyristoyl-, dipalmitoyl-, and distearoylphosphatidylcholines (DMPC, DPPC, DSPC, which only differ in the length of their hydrocarbon chains: 14, 16, 18, respectively) with incorporated mesoporphyrin (MP),[11] and adopted the method of site-selective fluorescence spectroscopy to learn more about the distribution of MP molecules. High-resolution spectroscopic investigation of such systems has not yet been reported. To avoid the difficulties arising from the differently protonated states of two propionate groups, we used the dimethyl ester of MP (MP-DME). By using different phosphatidylcholines, we sought to vary a single parameter: the length of the hydrocarbon chains. Because the applied method requires cryogenic temperatures ($\approx$10 K) and our measurements were unprecedented, we checked the quality of the liposome samples by dynamic light scattering (DLS) measurements after each step of the preparation and the experiment.

We demonstrate that the inhomogeneous distribution functions (IDFs) of MP in different liposome environments obtained from the fluorescence line narrowing (FLN) spectra are suitable for characterizing the location of MP molecules. On the basis of the analysis of these results, we identify the "spectral sites" with spatial locations in the liposome and provide evidence that supports our model.

Experimental Methods

According to some theoretical considerations and experimental experiences of porphyrin spectroscopy, in most cases the Soret band is not suitable for site-selective techniques.[27,28] The most appropriate transition for the determination of the IDF is the (1,m) $\leftarrow$ (0,0). Because of these we used the Q-band in our measurements, notwithstanding the fact that the molar extinction coefficient in this band is about 15 times less than in the Soret band. Moreover, because of the small capacity of the cuvette in the cryostat, we had to prepare a rather high concentration of MP sample to obtain a high enough signal for measurements. Thus, we prepared "quasi-saturated" samples producing well-defined comparable experimental conditions for all of the series of measurements (see below).

MP$-$Liposome Sample Preparation. Stock solution of mesoporphyrin IX dimethyl ester (MP-DME) (dimethyl 8,13-bis(ethyl)-3,7,12,17-tetramethyl-21*H*,23*H*-porphine-2,18-dipropionate; from Frontier Scientific, Inc., Logan, UT) was prepared in dimethylformamide (DMF) and kept in the dark to avoid photodegradation. The solution's concentration was approximately 1.7 mM. Hereafter we abbreviate MP-DME as MP for the sake of simplicity.

Different phosphatidylcholines (DMPC, DPPC, DSPC) (Sigma, St. Louis, MO) were dissolved in chloroform and then dried with a stream of nitrogen followed by placing in a vacuum ($\approx$2 Pa) for 15 min. Samples were kept in a desiccator at least for an overnight period. During this time the organic solvent nearly completely evaporated, and a thin lipid film formed on the vessel wall. Lipids were hydrated with phosphate-buffered saline (PBS) (10 mM phosphate, 137 mM NaCl, pH 7.4) at a temperature just above the main (liquid$-$gel) transition temperature (T_{m}) of the corresponding lipid membrane ($\approx$24, $\approx$42 and $\approx$55 °C, respectively). The samples were then sonicated twice for 10 min (MSE Soniprep 150 Ultrasonic Disintegrator, frequency 23 kHz; wave amplitude 8 μm), with a 5-min intermission to avoid excess heating. Remnants of multilamellar vesicles and contaminants (e.g., Ti particles from the sonicator) were removed by centrifugation (Beckman J2-21 centrifuge, 15 000 rpm, 25 min). The final phospholipid concentration was approximately 15 mM.

Porphyrin was added from stock to the liposome sample by mixing for 2 h. Glycerol, mixed in to a final concentration of 50% (v/v), was added for cryoprotection and to ensure transparency of the sample at low temperatures. For spectroscopic control of the samples at cryogenic temperatures, we monitored the shape of the fluorescence emission spectra of MP (see Figure 1). The spectra revealed the association process, and the saturation concentration was estimated as [MP]/[lipid] $\approx$ 0.003. We considered the sample to be "just saturated" at the MP concentration at which the unresolved part of the spectrum exactly vanished or appeared.

Addition of MP to the estimated saturating concentration usually does not yield a truly saturated sample because it takes more time to reach full binding equilibrium.[19] Such samples contain MP just below the saturation concentration; therefore, we refer to these as "quasi-saturated". Remnants of free MP (or its aggregated forms) did not disturb the fluorescence measurements because of the significant spectral separation from the emission maximum of associated MP (see Figure 1).

Addition of porphyrin to liposomes was usually performed at room temperature (RT $\approx$ 22 °C). In the case of DSPC, mixing was carried at a higher temperature as well (HT = 45 $\pm$ 1 °C, closer to $T_{\mathrm{m}} \approx$ 55 °C), so that additional controls may be carried

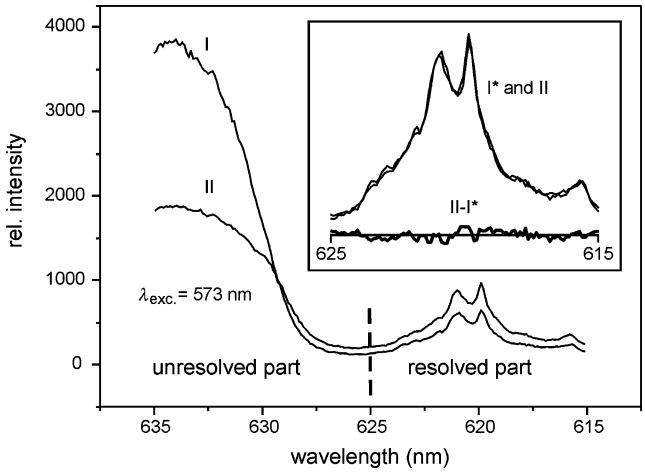

Figure 1. Broader range scan of fluorescence emission spectra of MP−DPPC (SUVs) in 50% (v/v) glycerol−PBS (pH 7.4) solution at 10 ± 1 K for samples with 4 × (I) and 2 × (II) of the estimated saturation concentration of MP, recorded by L1 luminometer (λ_{exc} = 573 nm). The broken line indicates the border of the unresolved and resolved parts of the spectra. The inset shows the (magnified) resolved part of the two spectra after an appropriate linear transformation applied to one of them (I*). The differential spectrum (II − I*) also is shown.

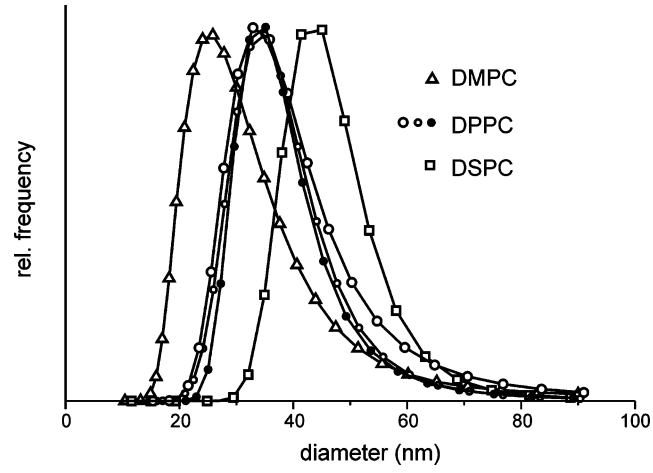

Figure 2. Size distribution obtained by dynamic light scattering (DLS) measurements for freshly prepared liposomes (small unilamellar vesicles, SUVs) from various phosphatidylcholines in PBS, pH 7.4: DMPC (△); DPPC (○, ◦, •, three different sample preparations, illustrating the reproducibility of the preparation); DSPC (□).

out. For high-temperature preparations a water bath set at 45 °C was used.

Following each step of the sample preparation the size distribution of liposomes was measured by dynamic light scattering (DLS). The mean diameter of the liposomes was in the 30−70 nm range, which is typical for small unilamellar vesicles (SUVs).

The final concentration of the samples was approximately 21 μM and 7.5 mM for MP and phospholipids, respectively. Spectroscopic measurements were carried out immediately following sample preparation.

Dynamic Light Scattering (DLS). DLS measurements were performed with equipment consisting of a goniometer system (ALV GmbH, Langen, Germany), a diode-pumped solid-state (DPSS) laser light source (Melles Griot 58-BLS-301, 457 nm, 150 mW), and a light detector (Hamamatsu H7155 PMT module). Prior to the measurement, the sample was diluted 10-fold with PBS. The different contributions of the autocorrelation function were determined by the maximum entropy method (MEM).[29] For spherical particles this contribution is proportional to the weight of the particle. In the case of unilamellar vesicles, this proportionality holds for r^2 as a good approximation, where r is the radius of the vesicle. With r^{-2} used as the weighting factor, the particle size distributions were determined. The MEM analysis software developed to evaluate the data is described elsewhere.[30]

Site-Selective Fluorescence Spectroscopy. All fluorescence measurements were carried out at 10 ± 1 K adjusted using a temperature-controlled closed-cycle helium cryostat (Cryophysics, Geneva, Switzerland). A series of fluorescence (line narrowing) emission spectra were recorded by scanning the wavelength over the inhomogeneous bands (603−627 nm) in steps matching the estimated spectral resolution (0.1 or 0.5 nm). The excitation wavelength was also varied in uniform steps (0.4 or 1 nm) in a defined range (555−584 nm). From the recordings, the inhomogeneous distribution function (IDF) was determined.

Fluorescence emission spectra were measured with two different luminometers (L1 and L2). Since we had very little initial information about the IDFs, we started the measurements with the L1 luminometer, which has a spectral resolution of about 0.1 nm. This spectrometer setup consists of a stabilized CW tunable ring dye laser (Coherent 899-01, Coherent Inc., Santa Clara, CA) with Rhodamine (6G) 590 (Exciton Co.) (line width better than 0.5 cm^{-1}) pumped by an Ar ion laser (Coherent Innova 307) (excitation side), a monochromator (Jobin-Yvon THR 1000, linear dispersion of 0.8 nm/mm) (emission side), and a cooled photomultiplier in photon counting mode (Hamamatsu R943-02).

Because the IDF turned out to be broad, and the lasing range of the dye is limited relative to this scale, a CD900 luminometer (L2) (Edinburgh Analytical Instruments, Edinburgh, U.K.) equipped with Xe lamp (75 W) excitation and photomultiplier detection (Hamamatsu R955) was used. The spectral resolution of this equipment is approximately 0.5 nm. The applicability of L2 was based on comparison of the IDFs obtained with the two luminometers (L1 and L2).

Spectra and IDFs were analyzed using the "Gaussian multipeaks fit" and "nonlinear curve fit" routines from Origin 7 software (OriginLab Corporation).

Results

Initial Sample Characterization. The homogeneity of the liposome samples was checked with dynamic light scattering (DLS). Figure 2 shows the size distribution of SUVs freshly prepared from various phosphatidylcholines in buffer solution. Small differences among the DPPC samples are clearly visible, illustrating the reproducibility of the preparation. The estimated modes (most probable values) of the diameters of the vesicles for hydrocarbon chain lengths 14, 16, and 18 are 25, 35, and 45 nm, respectively.

Figure 3 shows the effects of subsequent sample-preparation steps (MP addition, glycerol addition, low-temperature excursion) on the vesicle diameter in the case of DPPC. A shift in the size distribution of SUVs can be seen as a result of adding the estimated saturating amount of mesoporphyrin (MP). The mode of vesicle diameter is increased from 35 to 40 nm, but the distribution width remains unchanged. The full width at half-height (fwhh) remains about 16 nm. Upon glycerol addition the estimated mode of vesicle diameter (MP−DPPC SUV) increased from 40 to 50 nm, and a broadening of the distribution was

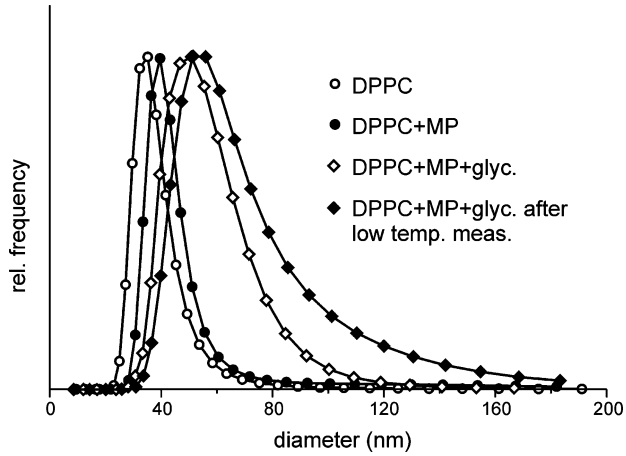

Figure 3. Size distribution obtained by dynamic light scattering (DLS) measurements for liposomes (SUVs) prepared from DPPC in four different cases: 1, freshly prepared SUVs in PBS, pH 7.4 (○); 2. after mesoporphyrin (MP) was added (until "quasi saturation") (●); 3 and 4, the MP−DPPC (SUV) sample in 50% (v/v) glycerol−PBS (pH 7.4) solution before (◇) and after low-temperature (10 ± 1 K) measurement (several hours later) (◆).

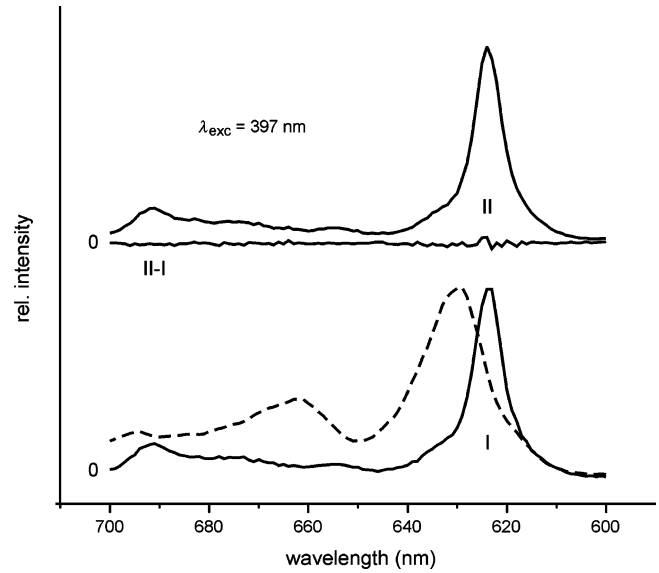

Figure 4. Normalized and shifted conventional fluorescence emission spectra of MP in various circumstances at room temperature (RT ≈ 22 °C) recorded at 397 nm excitation wavelength (in decreasing wavelength representation). (I) MP−DPPC (SUVs) in PBS (pH 7.4) solution, after it was mixed for 2 h ("quasi-saturated" sample; see the text). (II) MP−DPPC (SUVs) in 50% (v/v) glycerol−PBS (pH 7.4) solution, 35 min after the glycerol addition. Differential spectrum (II − I) is also shown. Spectrum of the same amount of MP in only 50% (v/v) glycerol−PBS (pH 7.4) solution can also be seen (broken-line curve).

also observed (fwhh increased from 16 to 30 nm). A further shift and broadening can be observed, which is most likely due to low-temperature excursion. The mode changed from 50 to 54 nm, and the fwhh changed from 30 to 35 nm. The change in size distribution caused by glycerol addition was more pronounced than that caused by low-temperature excursion.

Because SUVs may fuse, their MP content may also change. Therefore, we checked the effects of glycerol addition and low-temperature excursion with conventional fluorescence spectroscopy as well.

Figure 4 shows the normalized (and shifted) fluorescence emission spectra of MP in various circumstances at room temperature (RT ≈ 22 °C, 397 nm excitation wavelength). MP−DPPC (SUV) spectra prior to (I) and 35 min following (II) the addition of glycerol are almost identical. The difference spectrum (II − I) is essentially zero. Thus, glycerol addition did not significantly affect the amount of MP associated with liposomes. Had glycerol caused marked changes in MP association, significant spectral changes would have been observed (Figure 4, dashed line).

The initial measurements demonstrate that, although vesicle size distribution changes during glycerol addition and cryogenic cooling, liposomes are not destroyed and they preserve their MP content.

Concept of "Moderate Site Selectivity" and the Inhomogeneous Distribution Functions (IDFs). For high selectivity, a high-resolution luminometer with narrow bandwidth on the excitation and the emission sides (such as L1, see Experimental Methods) is required. Because of the limited lasing range of the dye laser and because initial results revealed a rather broad IDF, we used the lower resolution L2 luminometer for subsequent measurements. Reduced spectral resolution may cause closer lines to merge. To illustrate the effect of bandwidth, Figure 5A shows two spectra recorded at the same excitation frequency (17 452 cm^{-1} or 573 nm) marked with thinner and thicker solid lines corresponding to the higher (L1) and lower (L2) resolutions, respectively. In the lower resolution spectrum (L2), instead of double lines or line groups only broad "virtual" lines (or peaks) are observed. Equation 1 remains valid for these peaks because of the additive nature of light intensity. Although spectral resolution is partially sacrificed, the background correction becomes simpler and less ambiguous. Moreover, the larger signal results in an improved signal-to-noise ratio. Finally, the robustness of the IDFs obtained with either luminometers was comparable (see Figure 7C).

For the rest of the experiments, fluorescence emission spectra were recorded by the L2 luminometer at several excitation wavelengths in the 555−584 nm range for various MP−SUV samples. Emission peaks shifted according to the change of the excitation wavelength (Figure 5B), and the relative intensity of these peaks changed in accordance with the IDF of the MP molecules. Because of correlation between the actual excitation (ν_{exc}) and the nth peak frequencies (ν_n), the difference between them is constant, and the result is a typical vibrational frequency characteristic of the nth peak itself. Notably, because of the change in excitation frequency, some of the peaks leave the scanned range and others appear on the opposite side of the spectrum.

Figure 6 shows the spectrum marked with a thick solid line in Figure 5. We may identify three peaks specified by their characteristic vibrational frequencies. The three peaks and the background were fitted by four Gaussians under the assumption that the sum of independent phonon wings also follows normal distribution. After the first fit of all the spectra, when the fitted parameters were freely varied, a second fit was done with standardized widths of the individual peaks, which were estimated by averaging and were kept constant to reduce the number of free parameters. Ultimately each peak is characterized by two "changing" parameters, namely the position of the center of the actual peak (typical frequency ν_n) and the total area under the peak (proportional to the total emission intensity I_n).

After this fitting procedure, the frequency shift (due to the change of excitation frequency) and the change of the relative intensity of several emission peaks were monitored, and some $I_n(\nu_n)$ functions were determined. Figure 7A shows the change

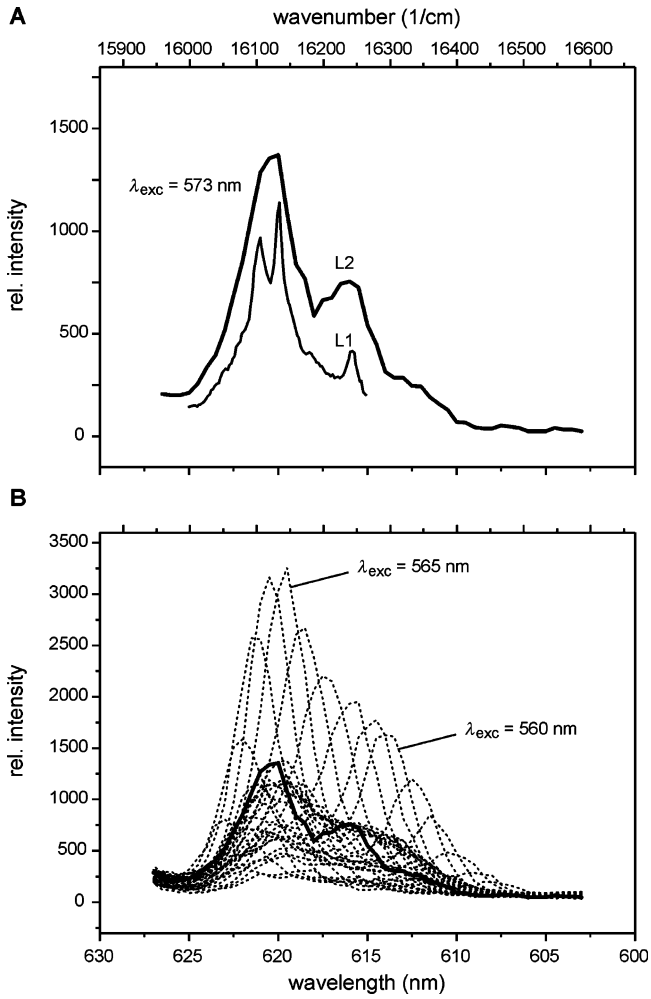

Figure 5. Fluorescence emission (line narrowing) spectra of MP−DPPC (SUVs) in 50% (v/v) glycerol−PBS (pH 7.4) solution at 10 ± 1 K in wavelength representation (bottom scale). Wavenumbers are also shown (top scale). (A) Effect of the increasing bandwidth: two spectra taken with 573 nm excitation are shown as thinner and thicker solid lines according to higher (≈0.1 nm) and lower (≈0.5 nm) resolutions, recorded by L1 and L2 luminometers, respectively. The less resolved spectrum is shown in (B) also, marked with a solid line and separately in Figure 6 with further explanations. (B) Series of spectra recorded by L2 luminometer. The excitation wavelength was varied in the 555−584 nm range (each step corresponds to 1 nm). Spectra marked with dotted line.

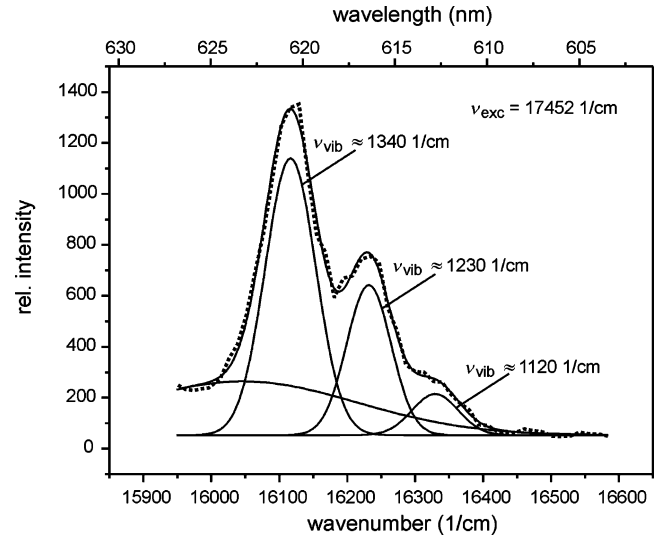

Figure 6. Fluorescence emission (line narrowing, ≈0.5 nm resolution) spectrum (dotted line) of MP−DPPC (SUVs) in 50% (v/v) glycerol−PBS (pH 7.4) solution at 10 ± 1 K, excited at 17 452 cm^{-1} (573 nm) (also shown in Figure 5) in wavenumber representation (bottom scale). Wavelengths are also shown (top scale). The fit by 3 + 1 Gaussians is also indicated (continuous line). Spectral peaks are marked with their characteristic vibrational frequencies.

of relative areas (total intensities I_n) of eight different peaks (n = 1,..., 8) plotted against the typical emission frequency (ν_n), marked with different symbols according to the characteristic vibrational frequencies. In such a series the same energy levels (marked with n) were excited, and neither the intensity (I_{exc}) nor the bandwidth ($\Delta\nu$) of the exciting light was changed. Based on eq 1 the intensity distribution will yield the number of excited molecules multiplied by a constant and a parameter, which is a representation of the inhomogeneous distribution function (IDF):

$$I_n = KI_{exc}AB_nN_0(\nu, \Delta\nu) = KI_{exc}AB_nN^*(\nu)\Delta\nu = K^*B_nN^*(\nu) \quad (2)$$

where K^* is a new constant and $N^*(\nu) = dN_0(\nu)/d\nu$ is the density function of the respective IDF. Naturally, the fluorescence emission probability (A) also is constant for all series, because of the common (1,0) → (0,0) transition. Differences in relative area among the eight series are a consequence of different intensities of spectral lines, arising from the different absorption transition probabilities which are taken into consideration by the B_n parameter. Their relative value was estimated by the total relative area under the corresponding series, and their inverse was used as a weighting factor for normalization. The normalized version of the eight series fitted with Gaussians is shown in Figure 7B. The final fitted curve is the best estimation of the IDF.

A higher resolution of the spectra did not provide a more reliable result for the IDF because of the more ambiguous fit results due to a more uncertain background correction (see Figure 7C).

Figure 8 shows four different IDFs in a simplified and standardized representation. Only some of the strongest lines (with smaller relative error) were used for evaluation, and their weighted average was taken for the plot. (Standard errors are comparable to the symbol size.). Open symbols and fitted lines mark the MP−SUV samples prepared at room temperature (RT ≈ 22 °C) from the three different phosphatidylcholines. Additionally, the fourth IDF for MP−DSPC prepared at higher temperature (HT = 45 ± 1 °C) is also shown (symbols without fit). It can be seen that this IDF of MP−DSPC is very similar to that of the MP−DPPC prepared at RT.

Discussion

According to our original purpose, we managed to determine the inhomogeneous distribution functions (IDFs) of MP incorporated in different liposomes (SUVs). Figure 8 can be considered as a summary of the presented site-selective fluorescence measurements. At first sight we can recognize the dual character of all IDFs. This fact gives the most demonstrative and direct evidence for the existence of two different and distinguishable populations of MP so far, which seems to be in agreement with some earlier results.[12,14,16]

Possible Interpretations and the Problem of Aggregation. An important question is whether the IDF is a consequence of different states of the dye molecule itself or of the environment of the dye. A possible change of the dye molecule itself could

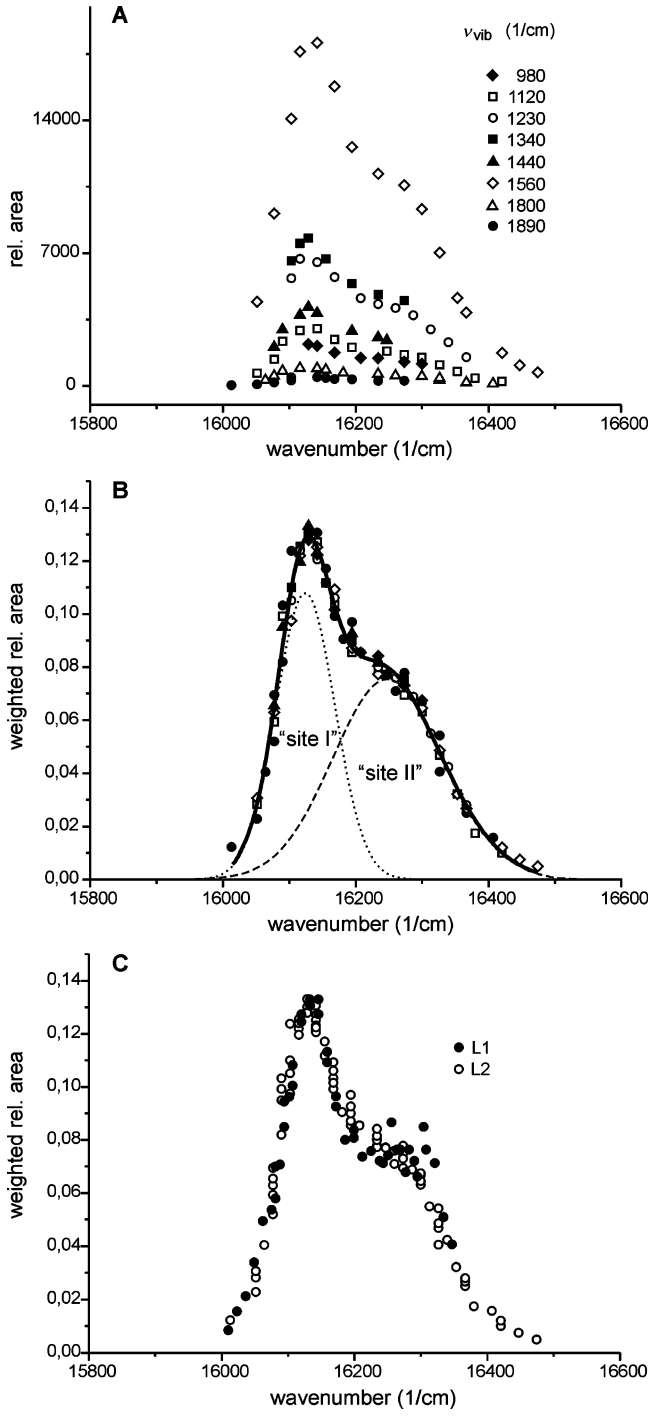

Figure 7. Determination of the inhomogeneous distribution function (IDF) of MP incorporated in DPPC liposomes (SUVs). (A) Changing areas (total intensities, I_n) of eight different peaks ($n = 1,..., 8$) (spectral lines or line groups, marked with different symbols according to different characteristic vibrational frequencies) as a function of the typical emission frequency (ν_n) (or wavenumber), varying due to the change of excitation frequency. (Differences among the eight series arising from the different absorption transition probabilities.) (B) Same series of peaks (lines or line groups, with the same symbols as in (A) after a weighting procedure (see text for more details) fitted with two Gaussians (dotted and dashed lines). The fitted curve is a representation of the IDF determined (solid line). (C) Two IDFs for comparison determined from data obtained with the two luminometers (L1 and L2).

be caused by the differently aggregated states of MP (e.g., monomers and dimers).

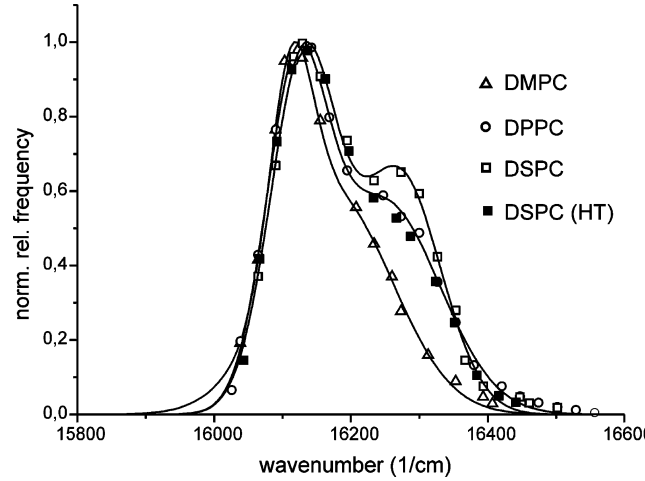

Figure 8. Inhomogeneous distribution functions (IDFs) of MP incorporated in different liposomes (SUVs) prepared at room temperature (RT $\approx$ 22 °C) from different phosphatidylcholines (in a simplified and standardized representation): DMPC (△, and fitted line); DPPC (○, and fitted line); DSPC (□, and fitted line). Additionally another IDF for DSPC prepared at higher temperature (HT = 45 ± 1 °C) is also presented (■, without fitted line).

There is earlier evidence that porphyrins tend to monomerize in the lipid phase,[7] but we wanted to provide direct experimental evidence for our specific case. In the beginning of our experiments, MP−liposome samples were prepared with various concentrations of porphyrin solution. Concentration was varied over 1 order of magnitude, and the greater part of this range was found above the estimated saturation concentration. We may assume that in these "saturated" samples the free but differently aggregated MP (monomer/dimer/.../multimer) was distributed in a different way at various concentrations. Therefore, the monomer/dimer/multimer ratios of MP should be different, at least outside the liposomes. Had there been differently aggregated MP associated with liposome, we should have seen differences in the respective parts of the spectra. However, the energy-selected fluorescence spectra of the associated MP were found to be very similar at various concentrations above saturation.

Figure 1 shows two spectra of MP−DPPC samples with about 4 × (I) and 2 × (II) of the estimated saturation concentration of MP in a broader range. We can easily distinguish the unresolved and resolved parts of the spectra, and we can identify them. The unresolved part of the spectra corresponds to the free but differently aggregated MP, while the resolved part of the spectra corresponds to the associated MP. For better comparison we have to take into consideration the differences due to the different baselines and the magnitude of signal. After an appropriate linear transformation applied to one of the spectra (I*), we obtained quasi-identical ones (see the inset in Figure 1; for better comparison, we also presented the differential spectra (II − I*)).

Thus, we may unambiguously rule out the notion that the IDF is caused by different aggregation states of MP associated with the liposomes. Rather, we attribute the components of the IDFs to MP in significantly different environments. These local environments can be identified with two distinguishable locations, which are also characterized by distributions.

Effect of Glycerol. Importantly, our samples contained glycerol. Therefore, all conclusions are valid only for such samples. The question is whether the presence of glycerol changes the location distribution of MP associated with liposomes or not. From dynamic light scattering (DLS) measure-

TABLE 1: Parameters of the IDFs Fitted by Two Gaussians: Center, fwhh (Full Width of the Peak at Half-Height), and Relative Area

		DMPC {14}	DPPC {16}	DSPC {18}	DSPC {18 HT}
"site I"	center (1/cm)	16112 ± 1	16119 ± 2	16130 ± 3	16125 ± 3
	fwhh (1/cm)	73 ± 6	104 ± 5	115 ± 6	109 ± 6
	rel area	0.25	0.44	0.54	0.46
"site II"	center (1/cm)	16175 ± 6	16248 ± 9	16270 ± 6	16247 ± 12
	fwhh (1/cm)	203 ± 7	194 ± 14	144 ± 11	189 ± 18
	rel area	0.75	0.56	0.46	0.54

ments we observed that glycerol alters the size distribution of the vesicles. Nevertheless, on the basis of some data provided in the literature, we can rule out liposome fusion as a possible reason for this change. Prior to each measurement we freshly prepared our samples and found, based on resonance energy transfer experiments, that glycerol reduces liposome fusion when its concentration exceeds 1 M.[31] Below the main (liquid−gel) transition temperature the change in the permeability of monocomponent liposomes (made from synthetic (dimyristoyl)lecithin, (dipalmitoyl)lecithin, and (distearoyl)lecithin, respectively) due to glycerol is negligible.[32] For some protein samples we found site-selective fluorescence spectra in different solvents, especially in PBS and in a 1:1 mixture of glycerol and PBS.[33] However, the two spectra differed only slightly.

We also checked the effect of glycerol addition by conventional fluorescence spectroscopy. Since the shape of emission spectra of MP did not change significantly upon the addition of glycerol (see Figure 4), we may conclude that the presence of glycerol does not significantly influence the amount of MP associated with liposomes. By using the site-selective fluorescence technique, which is much more sensitive than the conventional, we may draw further conclusions.

Although we could not measure site-selective spectra without glycerol, we could repeat our measurements with different durations of the mixing of the glycerol-containing samples. This waiting time until the beginning of the cooling process varied between about 5 and 35 min. On such a time scale the change of partition ratio among the possible locations of MP associated with liposomes would be observable if it occurred at all. As we mentioned in Experimental Methods, we checked all samples at low temperature by comparing the shapes of the fluorescence emission spectra of MP. We found that, independently of the mixing time of liposome solution with glycerol, the fluorescence emission spectra of MP for repeated measurements maintained their "real similarity". This means that the resolved part of the spectra after an appropriate linear transformation became quasi identical (see also Figure 1). Based on this reasoning, we may assume that the presence of glycerol does not significantly influence the partition ratio among the possible locations of MP associated with liposomes.

Further Analysis of Data. On the basis of the fitting procedure (see Figure 7), we may decompose all four IDFs into Gaussians. We shall call the first (dotted line) "site I" and the second (broken line) "site II". Because of the microenvironment of "site I" and "site II", porphyrin molecules provide lower and higher frequency optical signals according to the bigger and smaller spectral shifts, respectively. The results of the decomposition are shown in Table 1. Here the center of the peak is characteristic for the population of molecules distinct from the others. "fwhh" signifies the full width of the peak at half-height. This parameter measures the heterogeneity of a typical microenvironment of the porphyrin molecules. The relative area under the peak is proportional to the total amount of molecules associated with a certain site (see eq 1).

With the increasing length of the hydrocarbon chain from DMPC {14} to DSPC {18}, some definite changes can be read from Table 1. In the case of "site I" all the parameters become higher, but to a different degree. For "site II" the shift of the center is more pronounced than for "site I". However, the width and the relative area vary inversely.

The question is whether we can deduce any more details about these "sites" on the basis of the analysis of parameters. How can we identify the "sites" found in frequency space with the sites in real space?

Earlier Models at Molecular Level. In earlier works the location of a photosensitizer in the bilayer was characterized by the terms "near the polar heads",[12] "in the hydrophilic or hydrophobic region",[14] "in the inner or outer phospholipid monolayer",[16] and "vertical location".[17−19] Since the membrane is not a static construction, a possible interpretation of these terms is that there is a single parameter, namely the depth which can uniquely determine the location, and the dye molecules are assumed to remain more or less parallel to the hydrocarbon chains. If the dye molecule is amphiphilic in character, it is a plausible assumption. In this case, by varying the lengths of hydrocarbon chains between the tetrapyrrole ring and the carboxylate groups of modified porphyrins, it was proved that the hydrophobic part of the molecule tends toward a deeper position in the bilayer.[18,19] This tendency should be valid for any hydrophobic (small) molecules.

The protoporphyrin molecule has been shown to be deeply buried in hydrocarbon regions of the membrane.[10,34] We also learned that the binding constant of mesoporphyrin is greater than that of protoporphyrin.[35] Moreover, the mesoporphyrin IX dimethyl ester is probably a more hydrophobic molecule than its nonesterified form. Therefore, one can suppose that it is located in the hydrophobic region of the lipid membrane. In this case the presence of two distinguishable locations of MP molecules cannot be interpreted simply by their different depths in the lipid chain region. Therefore, if we assume that these molecules are distributed along the deepest position and the only parameter is the depth, they cannot produce a distribution function with two maxima.

New Interpretation of MP Association. We propose the following model for the distribution of MP in liposome membrane. MP is located within the membrane at two distinguishable sites. One site is between the two lipid layers, and the other site is along the hydrocarbon chains. The Gaussian "site I" corresponds to the sites between the two lipid layers ("perpendicular" sites) and "site II" corresponds to the sites along the hydrocarbon chains ("parallel" sites).

The length of carbon chains was used as the only variable among the different phospholipids. However, we had to take into consideration the fact that the length indirectly alters the flexibility and the order of membrane structure as well. On one hand, it is obvious that the longer the chain the greater its flexibility, hence more compliant the membrane structure. On the other hand, porphyrin was associated with the liposomes at

room temperature (RT ≈ 22 °C), i.e., below the main (liquid−gel) transition temperature (T_m) for all different phosphatidylcholine membranes (≈24, ≈42, and ≈55 °C, for DMPC {14}, DPPC {16}, and DSPC {18}, respectively). The difference between RT and the T_m, however, varies from ≈2 to ≈33 °C, suggesting that the longer the chain length the greater the membrane order. Nevertheless, these two characteristics, i.e., the flexibility and the order of membrane structure, differently influence the microenvironment of MP.

It is well-known that membrane order is connected to the trans−gauche isomerization of hydrocarbon chains. Far below the respective main transition temperature, most of the chains are in an all-trans state. As temperature approaches T_m, the number of gauche states increases. These states begin forming mainly at the ends of the chains. As a result, the degree of order of the microenvironment between the two lipid layers rapidly decreases with increasing temperature and, after reaching a certain level of disorder, it hardly changes. Therefore, the "perpendicular" sites ("site I") of MP are much less sensitive to changes in the general order of membrane structure than the "parallel" sites ("site II"). In addition, the location of MP in the "perpendicular" sites is inconceivable without flexibility, while this is not so crucial for "parallel" sites.

Let us consider again the parameters shown in Table 1 and compare them more carefully. As we mentioned earlier, the center of the peak is characteristic of the population of MP molecules distinct from the others. In the case of "site I" this parameter changes only slightly with increasing hydrocarbon chain length (from DMPC {14} to DSPC {18}), but in the case of "site II" it undergoes significant alteration. This must be a consequence of the "perpendicular" and "parallel" positions of MP molecules. The rather well-defined environment (end of the chains) for "site I", which hardly alters with considerable shift of MP molecules between the two lipid layers, depends only slightly on the length of the chains, while the environment for "site II" changes greatly with the shift of MP molecules along the chains and with the chain length as well. The fwhh parameters, which measure the heterogeneity of a typical microenvironment of the porphyrin molecules, support this argument, because these parameters for "site I" are considerably smaller than those for "site II" at any chain length.

Based on the preceding logic, the increase (for "site I") and the decrease (for "site II") of heterogeneity (fwhh) with increasing chain length (from DMPC {14} to DSPC {18}) become understandable. In the case of "site I" the flexibility is the determinant, and the change of order of the microenvironment is not significant. Thus, in a looser structure the environment is less defined and more variable. The increase of the relative area under the peak, which is proportional to the total amount of molecules associated with this site, is also a consequence of this looser structure. By contrast, in the case of "site II", where the order is the determinant, the increasing chain length induces a more ordered structure and accordingly fewer variants of the microenvironments which cause the narrowing of the distribution.

In a final check of our model, we prepared an MP−DSPC {18} sample associating the MP with the liposome at higher temperature (HT = 45 ± 1 °C), closer to its T_m (≈55 °C). The shorter chain length (at room temperature) could be simulated by this method. We expected that (at identical chain lengths) the closer the preparation temperature to the T_m the less ordered the membrane structure. Because of the shortening of the "effective" chain length, the membrane would also become less flexible and tighter. The result obtained for the IDF of this sample (see Figure 8 and Table 1) was convincing and confirmed our expectation. The IDF of MP−DSPC {18 HT} is really more similar to the IDF of MP−DPPC {16} prepared at RT than to the IDF of the original MP−DSPC {18}.

Conclusions

We applied the method of site-selective fluorescence spectroscopy to determine the distribution of mesoporphyrin (MP) associated with monocomponent, small, unilamellar vesicles (SUVs) formed of different phosphatidylcholines. In comparison with some other techniques, this method has the advantage that the detected signal comes from the molecules studied and not from externally added labels. In this way all the real sites of these molecules contribute to the measured optical signal. From the spectra we determined the inhomogeneous distribution functions (IDFs) of MP in different liposome environments. These distribution functions point to the presence of two different locations of MP. Based on the fit results of the decomposition of the IDFs into Gaussians, we provided a consistent interpretation of our results at the molecular level. That is, one of the locations for MP is between the two lipid layers, and the other one is along the hydrocarbon chains.

Acknowledgment. We are very grateful to John Kelly, Dr. Miklós Kellermayer, and Dr. Szabolcs Osváth for careful reading of the manuscript and to Rózsa Markács and Edit Komáromi for their technical assistance.

References and Notes

(1) Dougherty, T. J. *Photochem. Photobiol.* **1987**, *45*, 879.
(2) Henderson, B. W.; Dougherty, T. J. *Photochem. Photobiol.* **1992**, *55*, 145.
(3) Dougherty, T. J. *Photochem. Photobiol.* **1993**, *58*, 895.
(4) Niesman, M. R.; Khoobehi, B.; Magin, R. L.; Webb, A. G. *J. Liposome Res.* **1994**, *4*, 741.
(5) Bonnett, R. *Chem. Soc. Rev.* **1995**, *24*, 19.
(6) Ben-Hur, E.; Geacintov, N. E.; Studamire, B.; Kenney, M. E.; Horowitz, B. *Photochem. Photobiol.* **1995**, *61*, 190.
(7) Lang, K.; Mosinger, J.; Wagnerová, D. M. *Coord. Chem. Rev.* **2004**, *248*, 321.
(8) Hoebeke, M. *J. Photochem. Photobiol., B: Biol.* **1995**, *28*, 189.
(9) Reddi, E. *J. Photochem. Photobiol., B: Biol.* **1997**, *37*, 189.
(10) Ricchelli, F. *J. Photochem. Photobiol., B: Biol.* **1995**, *29*, 109.
(11) Bárdos-Nagy, I.; Galántai, R.; Kaposi, A. D.; Fidy, J. *Int. J. Pharm.* **1998**, *175*, 255.
(12) Angeli, N. G.; Lagorio, M. G.; San Román, E. A.; Dicelio, L. E. *Photochem. Photobiol.* **2000**, *72*, 49.
(13) Postigo, F.; Mora, M.; De Madariaga, M. A.; Nonell, S.; Sagristá, M. L. *Int. J. Pharm.* **2004**, *278*, 239.
(14) Ricchelli, F.; Jori, G. *Photochem. Photobiol.* **1986**, *44*, 151.
(15) Ricchelli, F.; Jori, G.; Gobbo, S.; Tronchin, M. *Biochim. Biophys. Acta* **1991**, *1065*, 42.
(16) Ricchelli, F.; Gobbo, S. *J. Photochem. Photobiol., B: Biol.* **1995**, *29*, 65.
(17) Gross, E.; Ehrenberg, B. *Biochim. Biophys. Acta* **1989**, *983*, 118.
(18) Lavi, A.; Weitman, H.; Holmes, R. T.; Smith, K. M.; Ehrenberg, B. *Biophys. J.* **2002**, *82*, 2101.
(19) Bronshtein, I.; Afri, M.; Weitman, H.; Frimer, A. A.; Smith, K. M.; Ehrenberg, B. *Biophys. J.* **2004**, *87*, 1155.
(20) Personov, R. I. In *Spectroscopy and excitation dynamics of condensed molecular systems*; Agranovich, V. M.; Hochstrasser, R. M., Eds.; North-Holland: Amsterdam, 1983; Chapter 10.
(21) Avarmaa, R. A.; Rebane, K. K. *Spectrochim. Acta* **1985**, *41A*, 1365.
(22) Personov, R. I. *J. Photchem. Photobiol., A: Chem.* **1992**, *62*, 321.
(23) Angiolillo, P. J.; Leigh, J. S., Jr.; Vanderkooi, J. M. *Photochem. Photobiol.* **1982**, *36*, 133.
(24) Koloczek, H.; Fidy, J.; Vanderkooi, J. M. *J. Chem. Phys.* **1987**, *87*, 4388.
(25) Herenyi, L.; Suisalu, A.; Mauring, K.; Kis-Petik, K.; Fidy, J.; Kikas, J. *J. Phys. Chem. B* **1998**, *102*, 5932.
(26) Rebane, L. A.; Gorokhovskii, A. A.; Kikas, J. V. *Appl. Phys. B: Laser Opt.* **1982**, *29*, 235.
(27) Vacha, M.; Machida, S.; Horie, K. *J. Lumin.* **1995**, *64*, 115.

(28) Vacha, M.; Machida, S.; Horie, K. *Chem. Phys. Lett.* **1995**, *242*, 169.
(29) Jaynes, E. T. *Phys. Rev.* **1957**, *108*, 171.
(30) Modos, K.; Galantai, R.; Bardos-Nagy, I.; Waschmuth, M.; Toth, K.; Fidy, J.; Langowski, J. *Eur. Biophys. J* **2004**, *33*, 59.
(31) Anchordoguy, T. J.; Rudolph, A. S.; Carpenter, J. F.; Crowe, J. H. *Cryobiology* **1987**, *24*, 324.
(32) De Gier, J.; Mandersloot, J. G.; Van Deenen, L. L. M. *Biochim. Biophys. Acta* **1968**, *150*, 666.
(33) Grubor, N. M.; Hayes, J.; Small, G. J.; Jankowiak, R. *Proc. Natl. Acad. Sci. U.S.A.* **2005**, *102*, 7453.
(34) Ricchelli, F.; Gobbo, S.; Jori, G.; Moreno, G.; Salet, C. *Eur. J. Biochem.* **1995**, *233*, 159.
(35) Kępczyński, M.; Pandian, R. P.; Smith, K. M.; Ehrenberg, B. *Photochem. Photobiol.* **2002**, *76*, 127.

JP9022184